J. Fluid Mech. (1982), *vol.* 119, *pp.* 283–296
Printed in Great Britain

Stationary waves in a laboratory flume

By P. McIVER
School of Mathematics, University of Bristol, England

(Received 24 April 1981 and in revised form 6 October 1981)

The formation of stationary waves in a laboratory flume is described, and possible mechanisms for their production discussed. In particular, an investigation is made of waves on supercritical streams. The mechanism for creating such waves involves frictional action through the boundary layers and an approximate equation describing this process is presented and shown to give qualitative agreement with observation.

1. Introduction

The appearance of stationary waves on subcritical streams is a well-known phenomenon and has been a troublesome feature of many laboratory water channels used for model testing. A considerable amount of research has been devoted to finding methods to suppress these waves and this can now be done quite effectively. It was partly with this in mind that the high-speed circulating water channel in the Department of Mechanical Engineering at the University of Liverpool (hereinafter referred to as the flume) was fitted with a tilting false floor; by tilting the false floor downwards in the direction of flow stationary waves at subcritical speeds are suppressed. That stationary waves can also appear on a supercritical stream is less well known, as they occur only over a narrow range of Froude numbers. It was discovered that the formation of such waves in the flume could be triggered by tilting the floor slightly towards the oncoming supercritical flow, that is in the opposite direction required to suppress waves at subcritical speeds. In particular, it was found that a large single elevation of the free surface would often be produced. The research described in this paper was begun with two aims. Firstly, to discover why the tilting of the floor produces waves; and, secondly, to determine if these waves resembled known travelling-wave solutions.

The changes required to produce stationary waves on a steady stream were first fully described by Benjamin & Lighthill (1954). For any steady two-dimensional flow over a horizontal bed the following three quantities are constant at any cross-section: the volume flux per unit width

$$Q = \int_{-h}^{\eta} u\,dy, \tag{1.1}$$

the mean energy per unit mass

$$R = \frac{1}{\eta + h}\int_{-h}^{\eta} \left\{\tfrac{1}{2}(u^2 + v^2) + g(y + h) + \frac{p}{\rho}\right\} dy, \tag{1.2}$$

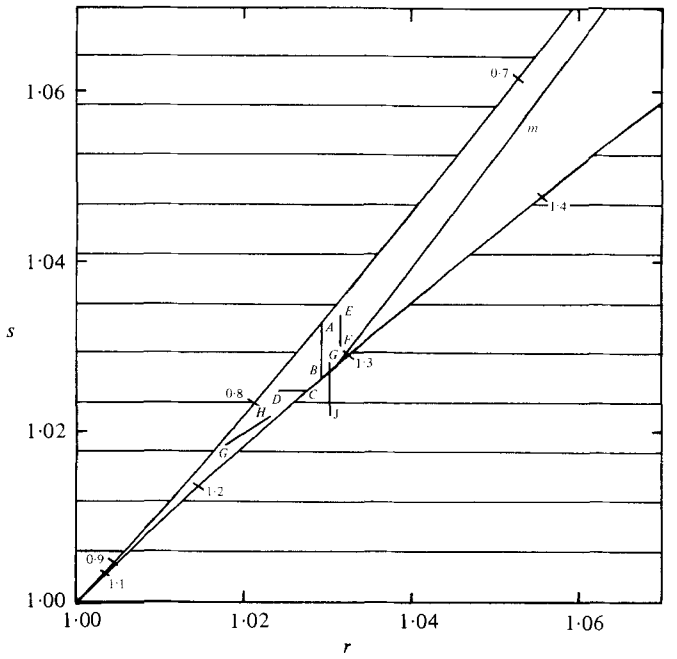

FIGURE 1. The (r, s)-diagram: see text for explanation of the lines AB etc.

and the momentum flux per unit width, corrected for pressure forces and divided by the density,

$$S = \int_{-h}^{\eta} \left(u^2 + \frac{p}{\rho}\right) dy. \tag{1.3}$$

Here y is the vertical coordinate, η the height of the free surface above the still-water level, and $y = -h$ is the bed of the stream. The horizontal and vertical components of velocity are denoted by u and v, the pressure by p, and ρ and g are respectively the density of the fluid and the acceleration due to gravity. Benjamin and Lighthill suggested that the values of Q, R and S determine a wave train uniquely, and proved that this is so for cnoidal waves. If the values of Q, R and S were known for all periodic gravity waves it would be possible to determine the changes in momentum and energy of a stream (the volume flux being constant) necessary to produce a particular wave train. With the use of computers it is possible to determine accurately the values of Q, R and S in terms of other wave parameters. The calculations for the solitary wave were made by Longuet-Higgins & Fenton (1974) and for the remainder of gravity waves by Cokelet (1977).

To make clear the kind of changes required to produce a particular wave train figure 2 of Benjamin & Lighthill's paper is reproduced here, in a slightly modified form, as figure 1. The dimensionless abscissa and ordinate are given respectively by $r = R/R_c$ and $s = S/S_c$, where R_c and S_c are the values taken by R and S for a critical stream of volume flux Q. The outer solid curves represent uniform flows, the subcritical flows ($F < 1$) lie on the left-hand branch and the supercritical flows ($F > 1$) on the right-hand. The numbers along the curve indicate the Froude numbers F. The right-hand branch also represents the solitary wave, it being the only wave that can arise from a

uniform stream without the action of friction. All other gravity waves lie within the cusped figure. The values of r and s within the horizontally shaded region do not correspond to steady flows; if a flow were to attain such values then some adjustment would take place until a point within the cusped figure was reached. A third barrier, the line within the cusp marked m, is that of those waves, close to the highest, for which r and s take their maximum values. (It was shown by Longuet-Higgins (1975) that the most energetic gravity wave was in fact not quite the highest.) Waves to the right of this barrier will break, thus reducing the energy to values in the unshaded region to the left of the barrier.

It is now a simple matter to deduce the kind of changes that can occur in a steady stream. The extraction of an increasing amount of momentum from a uniform subcritical stream will produce waves of ever greater length until a solitary wave is reached. Such a change is represented by the line AB in figure 1. Possible mechanisms for the removal of momentum are the lowering of an obstacle into, or the placing of an object on the bed of, the stream. If a small amount of energy is extracted from a uniform supercritical stream a wave very close to the solitary wave is produced. The line CD in figure 1 represents this process. Viscous forces, mainly due to the action of boundary layers, can provide the energy loss required to produce such a near-solitary wave. Experimental verification of this was found by Binnie, Davies & Orkney (1955) and Binnie & Orkney (1955). They found that a large wave would spontaneously appear on a supercritical stream when the Froude number was reduced below about 1·4. The wave closely resembled a solitary wave and was in fact the leading wave of an undular hydraulic jump (a stationary bore), their channel being of insufficient length to contain the remainder of the wave train. More recently, Sturtevant (1965) has demonstrated that, for bores travelling into still water, boundary-layer action is dominant in determining the properties of waves behind the bore front.

The appropriate periodic waves for shallow water are known as cnoidal waves, of which the solitary wave is the limit as the wavelength tends to infinity. Whitham (1974, p. 460) gives the background to the equations for these waves and shows how the first-order solution is found. Any small change in the energy and momentum flux of a uniform supercritical stream that gives a steady state will produce a wave close to the solitary wave. A slight tilt of the flume's false floor causes such a change. Hence a theoretical description of these changes is sought, based upon the assumptions of shallow-water theory.

2. Description of apparatus

The flume is a circulating water channel of approximate capacity 90000 l, with an axial flow impeller driven by a 75 kW motor. The working section has a length of 3·96 m, a width of 1·40 m and a maximum depth of 0·84 m. A false floor can be raised to reduce the depth to a minimum of 0·15 m; it can also be inclined from the horizontal. The flow velocity can be varied continuously in the range 0·03 m s^{-1} to 6·4 m s^{-1}.

Immediately before the working section, the flow is passed through a honeycomb, to reduce unevenness, and then accelerated through a contraction. An appreciable wake is cast off from the upper surface of the contraction; to compensate, additional water is introduced into the main flow at the free surface through a 1 mm wide slot running the breadth of the channel at the beginning of the working section. The rate of

injection can be varied to match the conditions of the main flow. At the downstream end of the working section the topmost layer of water is separated from the main flow by an adjustable flap. This water is slowed, allowing air bubbles caused by apparatus in the working section to escape, and then reintroduced into the main flow at a second adjustable flap.

The surface profile was measured by the use of a simple point gauge supported by a beam straddling the flume. Velocities were measured using a probe of the three-tube type (see Bryer & Pankhurst 1971, p. 60). This consists of a central Pitot tube and two chamfered side tubes each connected to a simple water-filled manometer. Such a device is particularly simple and easy to construct, consisting of three open-ended tubes soldered together with the tube axes in a single plane. The ends of the outer tubes were chamfered at an angle of 45° for maximum sensitivity to changes in the pressure. The probe is aligned with the flow by balancing the pressures in the outer tubes. This is known as the 'null-reading' technique. The total pressure can be measured directly from the centre tube. The static pressure, and hence the flow speed, is deduced from the difference in pressure between the inner and outer tubes using a previous calibration. The probe was attached to the end of a supporting stem or blade, streamlined so as to reduce the disturbance to the flow. The blade was not clamped rigidly into its mounting, but was able to respond to any changes of flow direction in the horizontal plane. Minor though these fluctuations are, experience with similar devices has shown that a rigidly mounted blade will bend owing to the lift generated once it ceases to be correctly aligned with the flow.

At a typical flow speed of 2 m s^{-1} it was estimated that the angle of flow was measurable to within 0·003 rad (about 0·2°) and the flow speed to within 0·02 m s^{-1}, an error of about 1 %. For further information on the calibration and performance of the velocity probe see McIver (1981).

3. Experimental results

To gain insight into the physical processes involved, a wide range of floor and speed settings were investigated. The results are summarized in figures 2–4. Three non-dimensional parameters are used; the wave amplitude a/h, the ratio of water depth to wavelength h/λ, and the Froude number F (measured at the channel inlet).

Figure 2 depicts the variation of amplitude with Froude number for a slope in the false floor of 0·002 rad. Results are included for a variety of depths, ranging from 0·4 to 0·8 m. Mostly the points lie close to a single line; that is the wave amplitude at a given Froude number varies little with depth. This does not necessarily mean that the same wave is obtained (waves referred to as the same occupy the same point in figure 1). Lines of constant amplitude arise from the right-hand curve of figure 1, and run in a direction roughly parallel to the left-hand curve, which itself corresponds to waves of zero amplitude. De (1955) gives a scaled form of Benjamin & Lighthill's diagram showing lines of constant amplitude and wavelength. Waves of the same amplitude in figure 2 could lie anywhere along such a line in figure 1.

The ratio of wave height to wavelength is plotted against Froude number in figure 3. Draw-down and non-uniformities at the channel exit usually meant there was no clearly defined downstream trough, making measurements of the wavelength unreliable. Caution should therefore be exercised when drawing conclusions from such

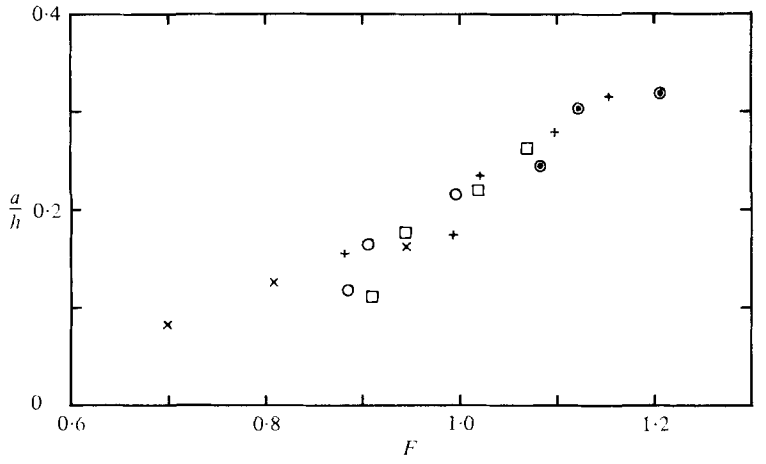

FIGURE 2. Variation of wave amplitude a/h with Froude number F for a bed inclination of 0·002 rad. Undisturbed water depth h: ×, 0·74 m; ○, 0·67 m; □, 0·58 m; +, 0·50 m; ⊙, 0·41 m.

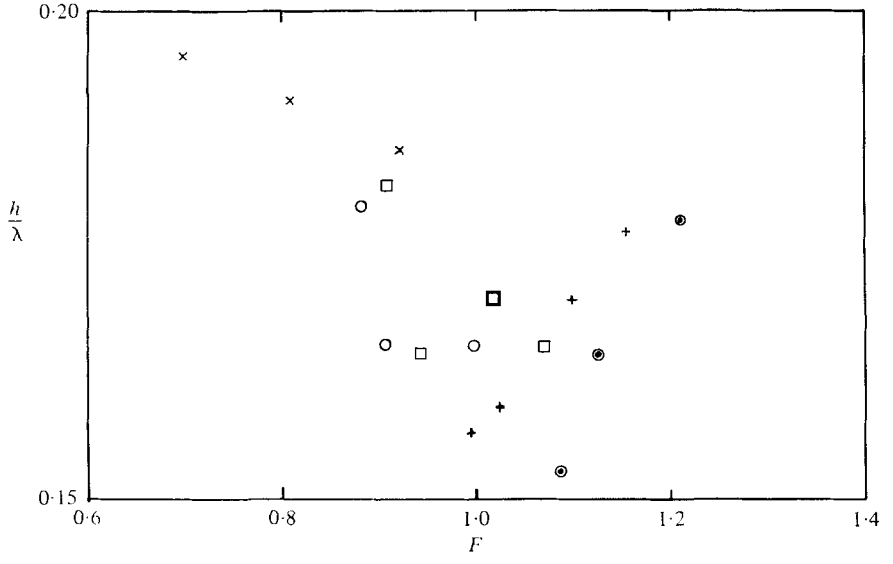

FIGURE 3. Variation of depth/wavelength ratio h/λ with Froude number F for a bed inclination of 0·002 rad. Undisturbed water depth h: ×, 0·74 m; ○, 0·67 m, □, 0·58 m; +, 0·50 m; ⊙, 0·41 m.

a diagram. However, as theory predicts, there is a trend for the longest wavelengths to occur at Froude numbers close to unity. The changes of wavelength with depth are uncertain; a tentative conclusion might be that there is a trend for longer waves to occur at shallower depth settings. This may be a consequence of the channel being effectively longer, allowing a wave to take up a more 'natural' configuration regarding the position of its nodes.

Figure 4 is similar to figure 2, but with results from three different inclinations of the false floor. The broken line satisfies the equation $F = (1+a/h)^{\frac{1}{2}}$, the first-order approximation to the solitary-wave celerity. Daily & Stephen (1952) showed that this formula is accurate to within about 2·5 % for travelling solitary waves up to an

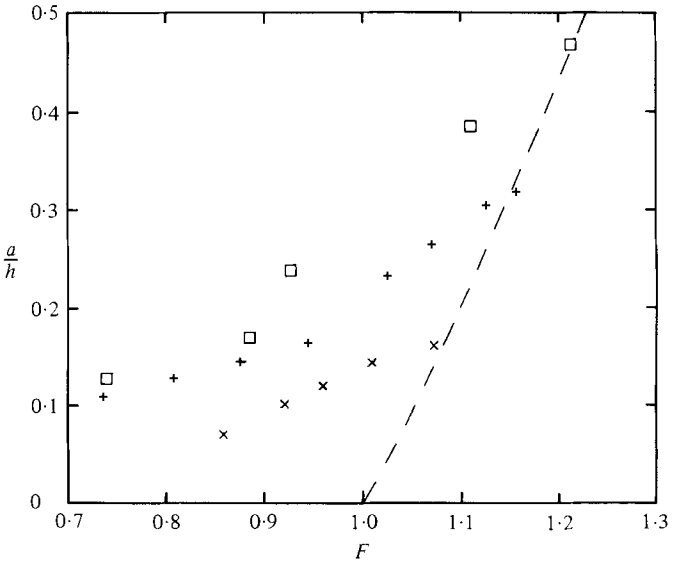

FIGURE 4. Variation of wave amplitude a/h with Froude number F for various bed inclinations: ×, 0·001 rad; +, 0·002 rad; □, 0·005 rad. The broken line satisfies $F^2 = 1 + a/h$, the first-order approximation to the solitary-wave celerity.

amplitude of about $a/h = 0{\cdot}6$. If figure 4 is compared with figure 3 of Binnie & Orkney (1955) a similar approach to the solitary-wave solution with increasing Froude number is found for spontaneous waves in a horizontal channel. Clearly it is close to this line that near-solitary waves can be expected to occur. The Froude number at the flume inlet would then be close to the non-dimensional wave speed, very little change in the original stream having occurred to produce such a near-solitary wave.

With the flow speed and the depth held constant, but the inclination of the bed increased, an increase in wave amplitude was generally observed. From Benjamin & Lighthill's diagram it seems that there are two feasible mechanisms that could cause such changes:

(i) the extraction of momentum, the flow changes being represented by a line like *EF* in figure 1;

(ii) the addition of both energy and momentum in such a combination as to produce changes similar to those represented by the line *GH* in figure 1.

The first alternative is the more likely, the greater area presented to the stream extracting additional momentum. If this is the case then for supercritical flows the waves at the low bed inclinations could not be solitary waves as further significant extraction of momentum would result in the flow point following a line like *IJ* in figure 1. The flow enters the shaded region, and steady waves can no longer occur. This deduction appears to be confirmed by the results of figure 4 for Froude numbers not much greater than one. The initial tilting of the bed for these slightly supercritical Froude numbers produces a wave considerably different from a solitary wave. However, it might have been anticipated that a solitary wave would be unobtainable in these circumstances. For non-dimensional wave speeds only slightly greater than unity the solitary wave has an effective wavelength significantly greater than the length of the flume working section. A wave would not be able to appear until changes in momentum and energy

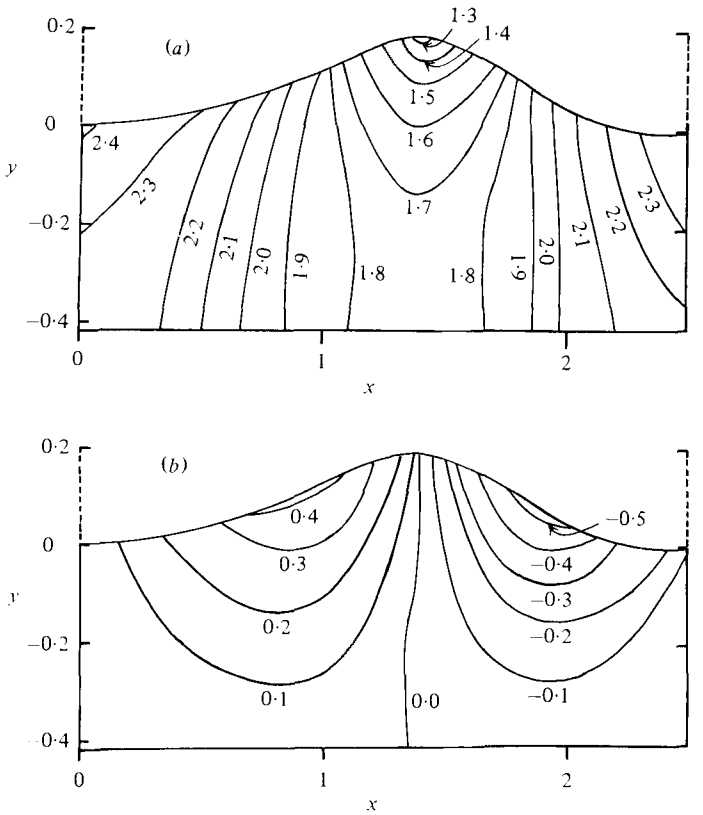

FIGURE 5. Horizontal (*a*) and vertical (*b*) velocity contours (data set *A*). Distances are in m and velocities in m s^{-1}.

capable of producing a wave of only moderate length had taken place. At shallower depths the greater effective length of the working section is offset by the proportionally greater effects of the sloping bed and boundary layers acting to give a wave not close to a solitary wave.

The second alternative for the creation of higher waves may also have a place. The increased tilt of the bed forces the waves to form closer to the channel inlet, the initial flow may be affected by this, the stream emerging under pressure and consequently with increased values of R and S. These increases were confirmed by experimental measurements for waves at steep bed inclinations.

In all, four sets of measurements were made of the velocity and the static pressure over a two-dimensional grid in a plane perpendicular to the bed and parallel to the flow direction. The full details of each data set are given in McIver (1981), some information from two of them will be presented here. Each set of measurements was made in water with an average undisturbed depth of 0·415 m. The first set, designated A, was made with a calibrated velocity setting of 2·425 m s^{-1} (the calibrated speed is that of the uniform flow obtained for a given rate of revolution of the flume impeller) and with the bed inclined at 0·0044 rad. The second set, designated B, has a calibrated velocity of 2·250 m s^{-1} and a bed slope of 0·0052 rad. The wave corresponding to A lies close to the solitary-wave line of figure 4, whereas B does not.

A representative set of velocity contours is displayed graphically in figure 5, the

x (m)	η (m)	Q (m^2 s^{-1})	R (J kg^{-1})	S (m^3 s^{-2})
0·00	0·000	0·978	6·831	3·142
0·20	0·006	0·976	6·828	3·132
0·35	0·017	0·981	6·827	3·141
0·50	0·032	0·980	6·825	3·130
0·60	0·045	0·981	6·820	3·127
0·70	0·061	0·987	6·820	3·135
0·80	0·081	0·988	6·830	3·137
0·90	0·102	0·994	6·841	3·147
1·00	0·123	0·994	6·847	3·147
1·10	0·145	0·994	6·845	3·139
1·25	0·175	0·994	6·823	3·121
1·40	0·186	0·991	6·833	3·120
1·55	0·167	0·987	6·862	3·127
1·65	0·143	0·973	6·854	3·097
1·75	0·115	0·977	6·854	3·098
1·85	0·086	0·965	6·847	3·070
1·95	0·057	0·945	6·870	3·040
2·05	0·031	0·922	6·816	2·967
2·20	0·005	0·902	6·820	2·924
2·35	−0·002	0·916	6·851	2·966
2·50	−0·002	0·930	6·803	2·976

TABLE 1. Data set A: η, Q, R, S. Calibrated flume speed = 2·425 m s^{-1}, slope of false floor = 0·0044 rad.

x (m)	η (m)	Q (m^2 s^{-1})	R (J kg^{-1})	S (m^3 s^{-2})
0·00	0·000	0·899	6·449	2·806
0·20	0·009	0·902	6·466	2·815
0·35	0·022	0·901	6·469	2·810
0·50	0·039	0·907	6·475	2·818
0·62	0·060	0·903	6·462	2·798
0·72	0·078	0·900	6·464	2·790
0·82	0·097	0·898	6·433	2·766
0·92	0·116	0·895	6·439	2·759
1·07	0·137	0·900	6·444	2·765
1·22	0·141	0·896	6·448	2·757
1·37	0·124	0·894	6·443	2·748
1·52	0·095	0·889	6·447	2·738
1·62	0·072	0·894	6·443	2·743
1·72	0·049	0·883	6·447	2·724
1·82	0·028	0·870	6·442	2·696
1·97	0·004	0·861	6·442	2·675
2·12	−0·012	0·853	6·438	2·655
2·32	−0·017	0·864	6·484	2·695

TABLE 2. Data set B: η, Q, R, S. Calibrated flume speed = 2·250 m s^{-1}, slope of false floor = 0·0052 rad.

flow direction is from left to right, with the origin of x corresponding to the beginning of the flume working section. Chebyshev polynomials were fitted to the measured surface profile using a least-squares method and the resulting smoothed profile is used in this figure and also for the subsequent calculations. A lack of symmetry in the profile is apparent; the water level at the downstream trough is lower than that at the channel inlet while the maximum slope of the downstream face is noticeably greater

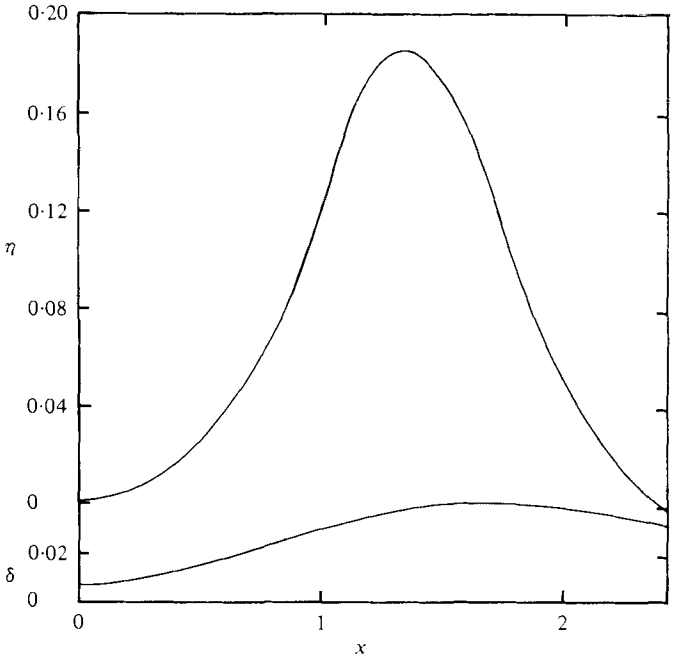

FIGURE 6. The boundary-layer thickness δ compared with the experimentally measured profile for data set A (distances in m).

than that of the upstream face. A corresponding asymmetry can be seen in the horizontal- and vertical-velocity contours; the whole wave appears to be tilted downwards in the direction of flow. A supercritical flow encountering a rise in the bed would experience a rise in the mean level. However, the Froude number of the flow over most of the length of the wave is less than unity, which perhaps explains this tilting of the wave.

The values of Q, R and S, as defined by (1.1)–(1.3) were calculated at a number of stations along the centre line of the flume, and are presented, along with the free surface height η, in tables 1 and 2. The integrations were carried out using Simpson's rule, and an approximation to the experimental error in Q, R and S was made by assuming that the error distribution within the summation can be approximated by a normal distribution. At the wave crest for data set A, for example, the errors are

$$\frac{\delta Q}{Q} \simeq \frac{0{\cdot}002}{0{\cdot}99} = 0{\cdot}002,$$

$$\frac{\delta R}{R} \simeq \frac{0{\cdot}009}{6{\cdot}83} = 0{\cdot}001,$$

$$\frac{\delta S}{S} \simeq \frac{0{\cdot}008}{3{\cdot}13} = 0{\cdot}003.$$

It is to be expected that the largest errors will occur at the wave crest, as it is here that the flow varies most rapidly with depth.

In calculating Q, R and S no account was taken of the bottom boundary layer. The extent of the boundary layer was determined by measuring the total head close to the bed and estimating where it attains its free-stream value. Figure 6 shows the experimentally measured boundary layer (for data set A) in relation to the free surface.

A crude estimate for the boundary-layer error can be made. Consider the energy per unit mass R, at any cross-section with a local depth h (assumed to be large compared with the thickness of the bottom boundary layer) and with hydrostatic pressure assumed,

$$R = \frac{1}{2h}\int_{-h}^{0} u^2\,dy + gh.$$

If the flow outside the boundary layer differs little from a uniform stream of velocity U then, to a first approximation,

$$\begin{aligned}\int_{-h}^{0} u^2\,dy &= U^2h - U^2\int_{-h}^{0}\left(1-\frac{u}{U}\right)dy - U^2\int_{-h}^{0}\frac{u}{U}\left(1-\frac{u}{U}\right)dy\\ &= U^2[h-(\delta_1+\delta_2)],\end{aligned}$$

where δ_1 and δ_2 are respectively the displacement and momentum thickness. Hence the error in R due to the boundary layer is given approximately by

$$\delta R = \tfrac{1}{2}U^2\bar{\delta},$$

where $\bar{\delta} = (\delta_1+\delta_2)/h$. Similarly, the errors in Q and S can be estimated respectively as

$$\delta Q = U\delta_1, \quad \delta S = U^2h\bar{\delta}.$$

For a turbulent boundary layer on a flat plate, Schlichting (1960, p. 536) gives

$$\delta_1 \sim \tfrac{1}{8}\delta, \quad \delta_2 \sim \tfrac{7}{72}\delta,$$

where δ is the boundary-layer thickness (the distance from the wall where the velocity reaches 99 % of its free-stream value). Beneath the wave crest for data set A the mean velocity is 1·65 m s^{-1}, and h and δ are respectively 0·6 m and 0·04 m. Hence the excesses in Q, R and S due to neglect of the boundary are given by

$$\frac{\delta Q}{Q} \simeq \frac{0{\cdot}008}{0{\cdot}99} = 0{\cdot}008,$$

$$\frac{\delta R}{R} \simeq \frac{0{\cdot}022}{6{\cdot}83} = 0{\cdot}003,$$

$$\frac{\delta S}{S} \simeq \frac{0{\cdot}026}{3{\cdot}13} = 0{\cdot}008.$$

This indicates that these errors are more significant than those due to inaccuracies in measurement; even so, they are small (less than 1 %) and less than the spread of values along the wave.

The results show a general trend for Q and S to decrease along the wave, though the behaviour of R is less clear. A decrease in R and S is to be expected because of the extraction of energy and momentum from the flow by the tilted floor and by viscous action. The decrease in Q, principally in the downstream third of the wave, indicates that fluid is being transported away from the centre of the channel by secondary flows. There are two possible types of secondary flow, the cross-flume motion caused by the differing shear stresses around the channel perimeter and also those generated by turbulence.

The flow at the downstream end of the channel is noticeably non-uniform across

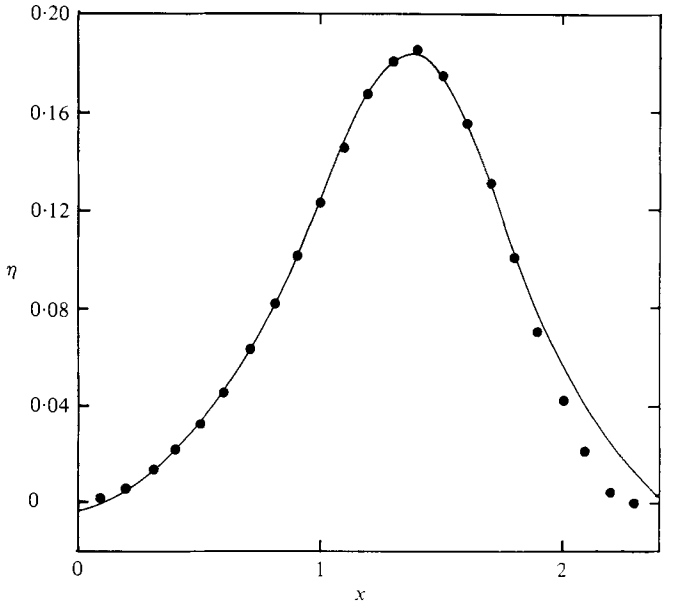

FIGURE 7. Free-surface height η: comparison of experiment with solitary wave for data set A (distances in m). Tilt = 0·07 rad (4°), a = 0·209 m, h = 0·396 m, c = 2·420 m s^{-1}.

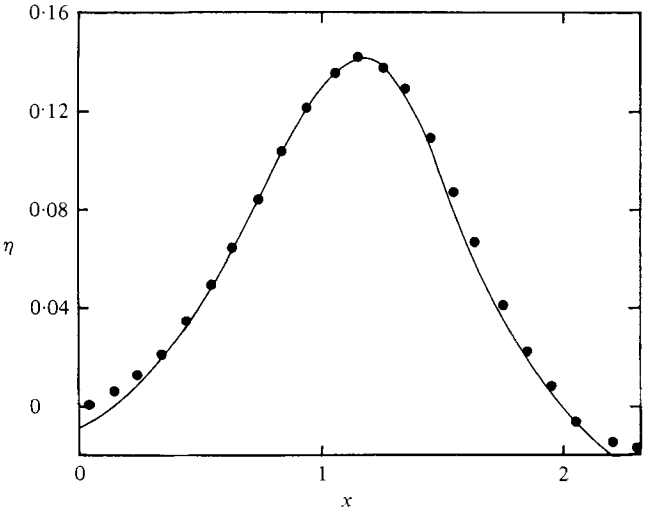

FIGURE 8. Free-surface height η: comparison of experiment with solitary wave for data set B (distances in m). Tilt = 0·05 rad (3°), a = 0·184 m, h = 0·378 m, c = 2·335 m s^{-1}.

the width, even away from the walls. With the highest waves there are deviations from the mean surface level, measured across the flume, of up to 1 cm. There are maxima in the height of the free surface at the walls and near the centre line, a further indication of the existence of secondary currents. In addition, in this part of the flume the free-surface height is slightly asymmetric about the centre line.

It is known that Q, R and S determine a wave train uniquely, so it should be possible to deduce the nature of a wave from their values. The spread in values along the wave necessitates some form of averaging. The cross-sections chosen for the measurements

have a greater density near the wave crest, so a simple average gives a weighting biased towards this region. The first thought is to compare the resulting values with those taken by solitary waves.

The distortion of the flow along the channel means that the wave height a and water depth h cannot be regarded as known, though their sum (the total depth below the crest) can. Using the third-order theory given by Fenton (1972), Q, R and S were calculated for solitary waves over a range of values of a and h such that $a+h$ retained its measured value. By comparing these calculations with the measured values an estimate was made for the true depth and wave height. The resulting solitary wave profiles and the measured profiles are compared in figures 7 and 8, the corresponding values of a, h and the wave speed c are given in the figure captions. As noted previously, the observed waves appear to be tilted slightly from the horizontal and the theoretical waves have been similarly inclined, in all cases by less than 0·07 rad (4°). When incorporated into the values of Q, R and S and $a+h$ the tilt affects only the third significant figure, which is within the limits required to determine a and h to within 0·005 m. Good agreement between theory and experiment is obtained, particularly in the first two-thirds of the wave. In the downstream third, secondary flows, and other effects of the finite-width channel distort the wave appreciably. Set A is closest to the solitary-wave line of figure 4, and gives the best agreement; note that the calculated wave speed is close to the calibrated flow speed. Set B is probably further into the cnoidal wave region, and will also be more distorted owing to the greater tilt of the false floor. Wiegel (1960) has given a detailed presentation of cnoidal wave theory; however, attempts to match with this proved unsuccessful, most likely because of the difficulty in obtaining a reliable wavelength.

4. Theory

Consider the steady flow of a uniform stream of speed U and depth h that encounters irregularities in the bed described by $y = b(x)$ (the origin of y is taken at the upstream level of the bed). If the changes in the bed level are small the velocity field may be considered as a uniform horizontal flow plus a small perturbation, described by the velocity potential $\phi(x, y)$. The solution of the problem for ϕ and $\eta(x)$ (the height of the free surface above $y = h$) may be carried out using a perturbation expansion of ϕ about its value on $y = 0$, similar to that used in solitary- and cnoidal-wave theory (see e.g. Whitham 1974, p. 464). To first order in the wave amplitude the equation for the free-surface height is

$$\tfrac{1}{6}h^2\eta_{xxx} + \frac{3}{2h}\eta\eta_x - (F-1)\,\eta_x + \tfrac{1}{2}b_x = 0, \tag{4.1}$$

where F is the Froude number of the upstream flow. Only second-order variations (relative to the wave amplitude) of the bed have been considered; with $b \equiv 0$ (4.1) is the Korteweg–de Vries equation for stationary waves.

A simple solution of (4.1) with non-zero b is found if

$$b = b_1 a \operatorname{sech}^2 \alpha x, \quad \alpha^2 = 3a/4h^3, \tag{4.2}$$

for some b_1, thus mimicking the solitary-wave profile. The solution is

$$\eta = a \operatorname{sech}^2 \alpha x, \quad a/h = 2(F-1) - b_1;$$

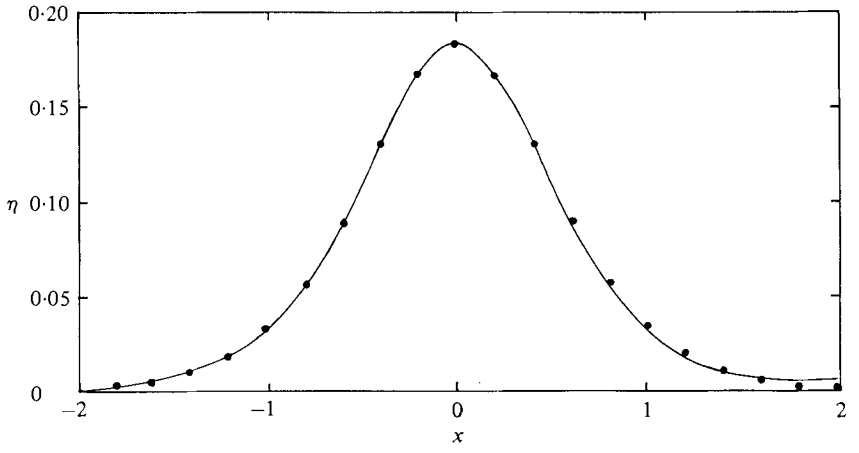

FIGURE 9. The solution of (4.1) with the measured boundary layer for wave *A* (——) compared with the first-order solitary wave (...). Distances are in m.

a solitary wave sitting over a slight hump on the bed will have an amplitude slightly less than that of a wave on a similar stream with a flat bed. A quantitative comparison of solutions of (4.1) with the experimentally measured profiles cannot be expected to be successful. The theory is applicable to flows with a Froude number little greater than unity, but shallow-water waves were only produced experimentally for these Froude numbers by tilting the false floor significantly, and hence violating the assumptions behind the theory. However, a qualitative test of the equation can still be made. The bed function $b(x)$ was chosen to represent the effects of the tilted bed and the bottom boundary layer together. The latter was achieved by estimating the displacement thickness from the boundary-layer thickness. Equation (4.1) was solved by a Runge–Kutta method using $\eta(-\infty) = 0$ as an initial condition. In figure 9 a comparison is made of the solution with the first-order solitary wave corresponding to the upstream conditions, the difference is negligible over the front face, but there is a slight increase in the slope of the rear face; this is in agreement with observation. The flow is from left to right.

5. Conclusion

The appearance of stationary waves in a laboratory flume, caused by the tilting of a false floor, has been explained in terms of changes in the energy R and the momentum flux S of the stream. The boundary layers appear to be of primary importance in bringing about the changes. It has been found that R and S can be measured with sufficient accuracy for them to be used as an aid in determining the nature of the waves. The profile of the irrotational solitary wave has been shown to give a good description of the free surface, even for stationary waves in a channel where viscous effects are important.

An existing theory for progressive waves has been adapted to describe the dissipation of energy by boundary layers in a steady flow. Qualitative agreement between theory and experiment has been found.

The author would like to thank Professor G. D. Crapper and Dr A. Millward for their guidance throughout the course of this work, and the Science Research Council for financial support. Thanks are due also to Dr E. J. Collins for his advice on the assessment of errors.

REFERENCES

BENJAMIN, T. B. & LIGHTHILL, M. J. 1954 On cnoidal waves and bores. *Proc. R. Soc. Lond.* A **224**, 448–460.

BINNIE, A. M., DAVIES, P. O. A. L. & ORKNEY, J. C. 1955 Experiments on the flow of water from a reservoir through an open horizontal channel. I. The production of a uniform stream. *Proc. R. Soc. Lond.* A **230**, 225–236.

BINNIE, A. M. & ORKNEY, J. C. 1955 Experiments on the flow of water from a reservoir through an open horizontal channel. II. The formation of hydraulic jumps. *Proc. R. Soc. Lond.* A **230**, 237–246.

BRYER, D. W. & PANKHURST, R. C. 1971 *Pressure Probe Methods for determining Wind Speed and Flow Direction.* London: H.M.S.O.

COKELET, E. D. 1977 Steep gravity waves in water of arbitrary uniform depth. *Phil. Trans. R. Soc. Lond.* A **286**, 183–230.

DAILY, J. W. & STEPHEN, S. C. 1952 The solitary wave. Its celerity, profile, internal velocities and amplitude attenuation in a horizontal smooth channel. In *Proc. 3rd Conf. Coastal Engng*, pp. 13–30. A.S.C.E.

DE, S. C. 1955 Contributions to the theory of Stokes waves. *Proc. Camb. Phil. Soc.* **51**, 713–736.

FENTON, J. 1972 A ninth-order solution for the solitary wave. *J. Fluid Mech.* **53**, 257–271.

LONGUET-HIGGINS, M. S. 1975 Integral properties of periodic gravity waves of finite amplitude. *Proc. R. Soc. Lond.* A **342**, 157–174.

LONGUET-HIGGINS, M. S. & FENTON, J. D. 1974 On the mass, momentum, energy and circulation of a solitary wave. II. *Proc. R. Soc.* A **340**, 471–493.

MCIVER, P. 1981 Stationary waves in open channels. Ph.D. thesis, University of Liverpool.

SCHLICHTING, H. 1960 *Boundary Layer Theory*, 4th ed. McGraw-Hill.

STURTEVANT, B. 1965 Implications of experiments on the weak undular bore. *Phys. Fluids* **8**, 1052–1055.

WHITHAM, G. B. 1974 *Linear and Non-Linear Waves.* Wiley.

WIEGEL, R. L. 1960 A presentation of cnoidal wave theory for practical application. *J. Fluid Mech.* **7**, 273–286.